Water adsorption on metal surfaces: A general picture from density functional theory studies

Sheng Meng,[1,2] E. G. Wang,[1] and Shiwu Gao[2]

[1]*Institute of Physics, Chinese Academy of Sciences, P.O. Box 603, Beijing 100080, China*
[2]*Department of Applied Physics, Chalmers University of Technology and Göteborg University, SE-412 96 Göteborg, Sweden*

We present a density functional theory study of water adsorption on metal surfaces. Prototype water structures including monomers, clusters, one-dimensional chains, and overlayers have been investigated in detail on a model system—a Pt(111) surface. The structure, energetics, and vibrational spectra are all obtained and compared with available experimental data. This study is further extended to other metal surfaces including Ru(0001), Rh(111), Pd(111), and Au(111), where adsorption of monomers and bilayers has been investigated. From these studies, a general picture has emerged regarding the water-surface interaction, the interwater hydrogen bonding, and the wetting order of the metal surfaces. The water-surface interaction is dominated by the lone pair–d band coupling through the surface states. It is rather localized in the contacting layer. A simultaneous enhancement of hydrogen bonding is generally observed in many adsorbed structures. Some special issues such as the partial dissociation of water on Ru(0001) and in the RT39 bilayer phase, the H-up and H-down conversion, and the quantum-mechanical motions of H atoms are also discussed.

PACS number(s): 68.43.Bc, 68.35.$-$p, 82.30.Rs

I. INTRODUCTION

Water interaction with solid surfaces[1,2] plays central roles in a variety of phenomena in nature such as catalysis, electrochemistry, corrosion, and rock efflorescing, and has important applications in, e.g., hydrogen production, fuel cells, and biological sensors. During the past two decades, water adsorption on single crystalline metal surfaces has been intensively investigated in laboratories by various experimental techniques[1,2] as a prototype system for understanding water-solid interfaces and their interactions. Depending on the coverage and experimental conditions, water on a surface forms different low-dimensional structures, ranging from isolated monomers and clusters, to one-dimensional (1D) chains, and two-dimensional (2D) ordered overlayers.[3] While the ordered 2D structures were accessible in earlier experiments by low-energy electron diffractions (LEED),[4,5] recent experiments using scanning tunneling microscope (STM) have made it possible to locally image and probe isolated water clusters. For instance, water monomers, dimers, and hexamers were recently observed by STM on Ag(111),[6] Cu(111),[7] and Pd(111) (Ref. 8) surfaces. A 1D water chain was observed on the steps of a Pt(111) surface.[3] As the coverage increases, water forms hydrogen-bonded (H-bond) networks of various phases, depending on the substrate, and continues to grow into multilayers and bulk ice at high coverages.[9]

What determine these adsorbed structures and their stabilities are the two fundamental forces at the water-metal interfaces, namely, (i) the water-surface interaction, which occurs predominantly in the water-metal contacting layer; and (ii) the interwater hydrogen bonding, whose character and strength may be modified by the presence of the substrates. On most metal surfaces, these two interactions turn out to be comparable in strength. Their competition results in a rich class of adsorbed structures especially at submonolayer coverages. Characterizing these structures, especially those at low coverages, is essential to the understanding of the water-surface interaction at the interfaces. Computer

simulation based on *ab initio* density functional theory (DFT) has proven to be a useful and supplemental tool to study the water-solid interfaces.[10]

Water on Pt(111) represents one of the most well studied systems by experiments, where various adstructures and vibrational spectra have been documented. Among all the structures, water bilayer in a $\sqrt{3} \times \sqrt{3} 30°$ (RT3) phase was first proposed by earlier experiments on the Pt(111) surface.[4] This bilayer phase is most interesting because it marks the initial formation of the H-bonded water networks on the surface. It has generally been observed on other metal surfaces such as Rh(111) (Ref. 11) and Au(111),[12] and has been viewed as a model water structure at the interfaces. In addition to the RT3 bilayer, two more bilayer phases, the $\sqrt{39} \times \sqrt{39} R 16.1°$ (RT39) and $\sqrt{37} \times \sqrt{37} R 25.3°$ (RT37),[13,9] have also been observed in recent experiments on Pt(111) at 130–140 K. These bilayers were found to be interconvertible at certain experimental conditions. Despite the tremendous experimental and theoretical efforts, our understanding on the simplest bilayer, the RT3 bilayer, remains to be controversial. While two RT3 bilayers, the H-up and H-down ones, were proposed in earlier experimental studies and a recent DFT calculation,[14] Ogasawara and co-workers argued in a recent experiment that only a flat bilayer of H-down type was observed in the RT3 phase on Pt(111) with a vertical O-O distance as small as 0.25 Å.[15] This conclusion has been recently questioned by Feibelman, who claimed that the wetting layer of the water/Pt should be the RT39 rather than RT3, based on the comparison of the adsorption energetics between the two phases.[16]

Besides the controversy in the bilayer, other nanostructures of water at surfaces such as monomers, clusters, and 1D chains, remain to be poorly understood due to their insensitivity to experimental probes and due to the fact that these nanostructures are computationally more demanding than the 2D periodic systems. Although recent STM experiments were able to image individual water clusters, it is difficult to determine the structure and bonding properties at surfaces because water molecules and clusters are usually very

mobile on the surfaces, even at temperatures as low as 10 K.[8] A particularly interesting type of water is the 1D water chains[3] on stepped surfaces, which resembles the 1D confined water in biomembranes. The latter has been investigated intensively in model confined geometries and nanotubes[17] by computer simulations. In contrast, the 1D chain observed on the Pt surface has been neither studied nor understood.

Another important and fascinating issue of adsorbed water is its dissociation and proton transfer at surfaces, where our understanding is far from conclusive. While water dissociation on oxide surfaces has been widely observed, water on metal surfaces is usually believed to be intact except when coadsorbed with other molecules or atoms.[1,2] However, a recent DFT calculation suggested that water bilayer on Ru(0001) is half dissociated with one OH broken.[10] This conclusion contradicts the conventional picture of molecular water on metal surfaces. Detailed vibrational spectroscopy using sum frequency generation has recently been carried out for water bilayers on Ru(0001).[18] The measured data compared well with the calculated vibrational spectra for molecular bilayers, suggesting that the water bilayer is undissociated. This issue remains unresolved and deserves our attention in future studies.

This paper presents a computational study of water adsorption on transition- and noble-metal surfaces using first-principles DFT calculations, with the goal to gain a general understanding of the water-metal interfaces and some of the issues mentioned above. First, various adsorption structures including water monomers, small clusters, 1D chains, bilayers, and multilayers, are investigated on the Pt(111) surface. The energetics of the adsorbed states, geometries, and vibrational spectra are determined and compared with available experiments. These results demonstrate the role of electronic structure in the water-metal interactions, as revealed by the interface charge transfer and H-bond enhancement, which in turn can be recognized vibrationally via the OH stretch mode. Some of the specific issues such as lattice mismatch, hydrogen disorder, partial dissociation, and the nature of the hydrogen bonding at surfaces, are investigated and discussed in detail. Second, the understanding gained on the Pt(111) surface is extended to other close-packed surfaces such as Rh(111), Ru(0001), Pd(111), and Au(111), adsorbed with two prototype structures: the monomers and bilayers. Correlation between the d-electron occupancy of the substrates and the structure and energetics of the adsorbed water molecules are illustrated. A simple picture of hydrophobicity and hydrophilicity, which was proposed in a previous study of water on Pt and Au,[19] is further examined and discussed. Besides, the vibrational spectra for the representative structures are given and provide a database for comparison with experiments.

The rest of this paper is organized as follows. With the introduction in Sec. I, computational methods and details are given in Sec. II. The main results are presented in Sec. III for water on Pt(111) and for monomers and bilayers on different metal surfaces. Vibrational spectra are also presented. Section IV focuses on a few specific issues such as the nature of the H bonding at surfaces, the H-up and H-down conversion,

TABLE I. The calculated and experimental lattice constants (Å) for several hcp (Ru) and fcc (Rh, Pd, Pt, Au) metals.

	Ru	Rh	Pd	Pt	Au
Theor.	2.72	3.83	3.96	3.99	4.18
Expt.	2.71	3.81	3.89	3.92	4.08

and partial dissociation of water bilayers. A short summary and conclusions are given in Sec. V.

II. COMPUTATIONAL METHOD

The calculations were carried out with the Vienna *ab initio* simulation program, VASP,[20] which enables us to do both structure optimization and molecular dynamics (MD) simulations. The metal surfaces were modeled by a supercell that contains a slab of typically four to seven layers of metal atoms and a vacuum region of ~ 13 Å. Water molecules were put on one side of the slab to simulate the adsorbed systems. The lattice constants of the surfaces were determined from bulk calculation and usually agree well with the experimental values (Table I). Different supercells, 3×3 and $2\sqrt{3} \times 2\sqrt{3}R30°$ for small water clusters and a $\sqrt{3} \times \sqrt{3}R30°$ cell for the RT3 overlayer, were calculated. The sizes of these unit cells are large enough to yield results close to convergence, with a typical accuracy around 5–10 % in energetics. Monkhorst-Pack scheme[21] with $3 \times 3 \times 1$ and $5 \times 5 \times 1$ k-point sampling in the surface Brillouin zone were used for the two sizes of supercells, respectively. A single Γ point sampling was adopted for large supercells including 1D water chains, the RT39, and the RT37 overlayers on Pt(111). A plane-wave cutoff at 300 eV was used in most calculations, while a higher cutoff of 400 eV was also performed to check convergence. The Fermi level was smeared by the Methfessel and Paxton[22] approach with a Gaussian width of 0.2 eV. The free energy was extrapolated to zero kelvin to yield total energies of the systems. This set of parameters assures a total energy convergence of 0.01 eV/atom.

In structural search, the water molecules and the surface layer of the slabs were relaxed simultaneously, while the bottom layers were fixed at their bulk positions. The search was stopped when the forces on all relaxed atoms were smaller than 0.05 eV/Å. In MD simulations, the molecules and the surface layer atoms were allowed to move according to the forces calculated from the converged electronic structure. A 300 eV cutoff in plane-wave basis and a time step of 0.5 fs were utilized in all MD simulations. To obtain the vibrational spectra, a 2 ps production run at 90–140 K was performed after equilibrating the system for ~ 1 ps. The vibrational spectrum was obtained from the velocity-velocity autocorrelation function in the MD simulation. Higher energy cutoff at 400 eV and a shorter time step of 0.25 fs did not change the peak positions or the shape of the vibrational spectra.

Reaction barriers were calculated by the nudged elastic band method,[23] available in VASP. For searching the minimum energy reaction pathway, this method employs a

TABLE II. The calculated geometries and energies of a free water monomer and a dimer. The bond angles (α, β) are as depicted in Fig. 1. The experimental data are taken from Refs. 28 and 29.

		Theor.	Expt.
Free H$_2$O	OH bond length (Å)	0.973	0.957
	HOH bond angle (deg)	104.85	104.52
	Dipole moment (D)	1.856	1.855
Free H$_2$O dimer	OO distance (Å)	2.86	2.98
	α (deg)	2.79	-1 ± 6
	β (deg)	126.35	123 ± 6
	Formation energy (kJ/mol)	24	23

constrained minimization of the total free energy of a trial path by relaxing a number of "images" in the path. All the water molecules and the surface-layer atoms were relaxed under the constraint, as in the ground-state optimizations.

The adsorption energy for an adsorbed water structure, E_a, has been defined as the mean adsorption energy per molecule of the adstructure,

$$E_a = (E_{\text{metal}} + n \times E_{\text{H}_2\text{O}} - E_{(\text{H}_2\text{O})_n/\text{metal}})/n. \qquad (1)$$

Here $E_{(\text{H}_2\text{O})_n/\text{metal}}$ is the total energy of the adsorption system, E_{metal} and $E_{\text{H}_2\text{O}}$ are those for the surface and free molecules, respectively, and n is the number of water molecules in the cell.

In our calculations, the Vanderbilt ultrasoft pseudopotentials (USPP) (Ref. 24) and the generalized gradient approximation (GGA) for the exchange-correlation potential by Perdew and Wang (PW91) (Ref. 25) were used. The GGA extension is crucial for the accurate treatment of the hydrogen bonds and water structures.[26] The PW91 form has been tested extensively for a variety of intermolecular interactions including H bonding.[27] To illustrate the feasibility of the USPP+PW91 approach for describing water and hydrogen bond, the calculated geometries and energetics of a free water molecule and dimer were tabulated in Table II. The OH bond length and dipole moment of the monomer, and the geometry and formation energy of the dimer, show excellent agreement with experiments. Moreover, the vibrational spectrum obtained from MD for a free water dimer (Fig. 1) also agrees well with other calculations and experiments.[28,29]

III. RESULTS

The first part of this section presents results of water adsorption on Pt(111) in various phases including monomers, clusters, and overlayers. The structures, energetics, and the interaction between water molecules and the substrate are studied in detail. The second part extends this study to other metal surfaces, where general features of water adsorption and the effect of different substrates are investigated. Vibrational spectra obtained from the simulations are given in
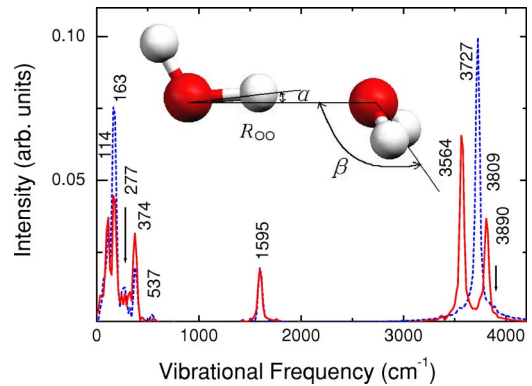
FIG. 1. Vibrational spectrum for a free water dimer. Solid and dashed lines correspond to the proton donor and acceptor, respectively. The inset shows the optimized geometry of the dimer.

the last part, providing a database for comparison with experiments.

A. Water adsorption on Pt(111) surface

1. Water monomers on Pt(111)

The adsorption of water monomer contains the essential information regarding the water-metal interaction, and has been investigated first. Structure optimization and energetics indicate that adsorption on top site [see Fig. 2(a)] is most stable compared to bridge and hollow sites (Table III). This is further supported by a shorter H$_2$O-metal (O-M) bond length on the top site ($d_{\text{OM}} = 2.43$ Å). Water lies almost flatly on the surface with its polar axis making a small angle $\theta = 13° - 14°$ with the surface plane. The OH bond is stretched slightly, while the HOH angle is more open than the free water molecule (0.973 Å and 104.85°, Table II). These results indicate electron transfer from O to surface atoms. Although the top site adsorption has been found in most recent studies, bridge site with an upright geometry was also reported for monomer in an earlier study.[30] Our calculation shows that the upright configuration is 40 meV unfavorable compared to the flatly adsorbed monomer on the bridge site. More accurate results with a six-layer Pt slab and a higher-energy cutoff (400 eV) are also given in Table III, which shows minor variations in the structure ($\sim 1\%$) and adsorption energy ($\sim 3\%$) for the adsorbed monomer.

To gain insight into the dynamics of the adsorbed monomer, the distance- and angular-dependent energies of the
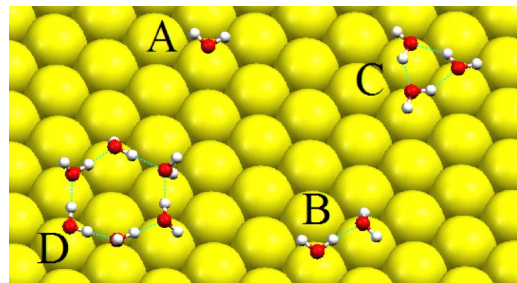
FIG. 2. The water monomer and small clusters adsorbed on the Pt(111) surface.

TABLE III. Water monomer adsorption on the (111) surface of Pt. Energies, distances, and angles are in units of meV, Å, and deg, respectively. Results for different Pt layers in the slab and energy cutoff are shown for comparison.

Layers	E_{cut} (eV)	Top		Bridge		Hollow		d_{OH}	$\angle HOH$	θ
		d_{OM}	E_a	d_{OM}	E_a	d_{OM}	E_a			
4	300	2.43	291	3.11	123	3.12	121	0.978	105.36	13
6	400	2.40	304	2.89	117	3.02	102	0.980	105.62	14

H_2O/Pt(111) are plotted in Fig. 3, as functions of the O-Pt distance d_{OPt} and the bending angle θ. The distance dependence (left panel) shows an equilibrium bond length at 2.43 Å for the O-Pt bond. In the angular dependence, $\theta = 0$ corresponds to the molecule lying down on the surface, while $\theta = 90°(-90°)$ corresponds to the upright position with the O atom pointing toward (away from) the surface. The energy profile was obtained by rotating H_2O molecule while keeping O fixed at its equilibrium position. The rotational barrier at $\theta = 90°$ is 140 meV, lower than what Michaelides and co-workers[31] reported recently, ~ 190 meV. The discrepancy might result from the smaller supercell, 2×2, used in their calculation. (Our calculation used a 3×3 supercell.) In addition, the rotational barrier along the azimuthal angle is found to be very small (less than 2 meV), which suggests that water molecule can rotate freely on the surface. We can conclude from these results that the adsorbed monomer can rotate freely in two dimensions on the surface. The bending motion could also be quite active near the equilibrium angles.

2. Water clusters on Pt(111)

The adsorption of water clusters is interesting because both the H bonding and water-surface interactions are involved in the adsorbed clusters. Studying these clusters at surfaces may help us understand the competition between the two interactions at low coverages. On metal surfaces, water clusters were observed by a number of experimental techniques such as high-resolution electron-energy-loss spectroscopy (HREELS),[32] infrared adsorption spectroscopy,[33] He atom scattering (HAS),[34] and STM.[6,8] On Pt(111), water dimers, trimers, and other clusters were identified by vibrational spectroscopies.[34,35] Yet their detailed structures and bonding properties have not been determined by experiments so far. We calculated water dimers, trimers, and hexamers adsorbed on Pt(111). A supercell of 3×3 was employed for dimer and trimer adsorption, while a larger cell of $2\sqrt{3} \times 2\sqrt{3}$ was used for hexamers. The obtained structures are depicted in Fig. 2. The energetics and geometric configurations for each molecule in the clusters are specified in Table IV.
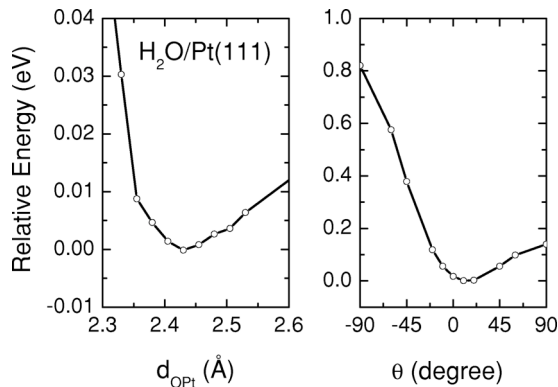
Generally speaking, the geometries of these clusters look quite similar to their gas-phase counterparts.[36] Water molecules prefer atop site adsorption, whenever possible. They tend to lie down onto the surface, due to the cluster-surface interaction. In the dimer case, for example, both the proton donor and acceptor take an atop site as shown in Fig. 2(b), although the donor couples more strongly to the surface than the acceptor, forming two O-Pt bonds (with $d_{OPt} = 2.26$ and 3.05 Å, respectively) plus an internal H bond. Besides the difference in O-Pt bond length, the donor and acceptor also differ in other details. The geometry of the donor is quite similar to that of the adsorbed monomer with $\theta = 25.1°$, while the acceptor lands onto the surface with $\theta = -41.8°$. The donor and acceptor make thus an angle β of around 120°, as in the free dimer. The O-O distance, $d_{OO} = 2.70$ Å, is shortened (2.86 Å for the free dimer, Table II); and the OH bond is stretched slightly (1.012 Å, compared to 0.985 Å for the free dimer). One can thus infer that the H bond in the adsorbed dimer is enhanced. A wider $\angle HOH$ in

FIG. 3. The variation of the total energy for a water monomer on Pt(111) as a function of the H_2O-Pt distance d_{OPt} (left panel) and the tilt angle θ (right panel).

TABLE IV. The adsorption energies and geometries for small water clusters on Pt(111). Energies, distances, and angles are in units of meV, Å, and deg, respectively.

Cluster	E_a	d_{OPt}	θ	d_{OH1}	d_{OH2}	$\angle HOH$	d_{OO}
Monomer	304	2.40	13.8	0.980	0.980	105.62	
Dimer	433	2.26	25.1	0.978	1.012	106.72	2.70
		3.05	41.8	0.981	0.982	103.52	
Trimer	359	2.76	3.5	0.975	0.985	107.75	2.78
		2.76	3.5	0.975	0.985	107.86	2.80
		2.76	3.1	0.974	0.985	107.71	2.79
Hexamer	520	2.32	31.1	0.997	1.001	106.22	2.99
		3.38	32.9	0.974	0.991	104.49	2.80
		2.77	1.8	0.978	0.990	107.25	2.89
		3.35	0.3	0.975	0.988	106.88	3.01
		2.77	3.7	0.979	0.987	107.14	2.80
		3.39	32.3	0.974	0.991	104.83	2.88

the donor and a narrower $\angle$HOH in the acceptor are also observed, which may be caused by electron transfer from the donor to the substrate and the back donation from the substrate to the acceptor, due to the interactions with the surface.

The trimer and hexamer retain their ringlike structures. Each molecule in the trimer lies very flatly ($\theta \sim 3.5°$) on the surface, with one OH forming an H bond and the other being free, as shown in Fig. 2(c). Cyclic hexamer forms a puckered hexagonal ring with three molecules lying closer to the surface (d_{OPt}=2.32, 2.77, 2.77 Å). The other three are a little higher ($d_{OPt} \sim 3.4$ Å). The adsorbed hexamer thus form 3 O-Pt bonds and 6 H bonds. One water molecule is a double proton donor, and lies much close to the surface. The averaged O-O distance is slightly larger than that of the free dimer and trimer. In the gas phase, there are two additional hexamer structures, the cage and prism hexamers.[36] The adsorption energy for the prism structure on Pt is 321 meV, which is 200 meV lower than the cyclic hexamer. So it may not exist on the Pt surface.

Among these clusters, cyclic hexamer is most stable with adsorption energy of 520 meV per molecule. The trimer is least stable with an adsorption energy of only 359 meV. The adsorption energy of the dimer, 433 meV, lies in between. This energy difference reflects dominantly the variation in the number of water-metal bonds and the H-bonds formed in the adsorbed clusters. Compared with experiments, cyclic water hexamer was already observed by STM experiments on Ag(111),[6] Cu(111),[7] and Pd(111) (Ref. 8) surfaces, although no experiment has been available on Pt(111). Small clusters including dimers and trimers were also reported on Pd (Ref. 8) by STM, formed via diffusion of monomers.

3. One-dimensional water chains on Pt steps

The 1D water chain is an interesting type of structure, because it is believed to exist in the water pores across biomembranes. It also provides an ideal 1D model system based on water molecules. Modeling the structure and dynamical properties of 1D water has been carried out intensively for water confined in carbon nanotubes[17] and model confining potentials. Such 1D model structures have neither been observed nor realized by any experiments so far. The 1D water chain found experimentally on the steps of the Pt surface[3] is therefore extremely interesting and has been studied in our calculation. To model the $\langle 110 \rangle / \{100\}$ step found in the experiment,[3] a slab with 15 layers of Pt in a (322) surface is used in the calculation. The unit cell is schematically shown in Fig. 4. The water at the step can form different chain structures depending on the H bonding and OH orientations at the step. The two simplest water structures are the ones shown in Fig. 4, where one OH of each water connects the chain and the other OH bond points either inward [H-in, molecule 1 in Fig. 4(b)] or outward (H-out, molecule 2). A zigzag chain, with one H-in molecule coupled alternatively to an H-out molecule, has also been calculated [Fig. 4(b)]. The results for the three calculated structures are given in Table V. For comparison, monomers adsorbed in the H-in
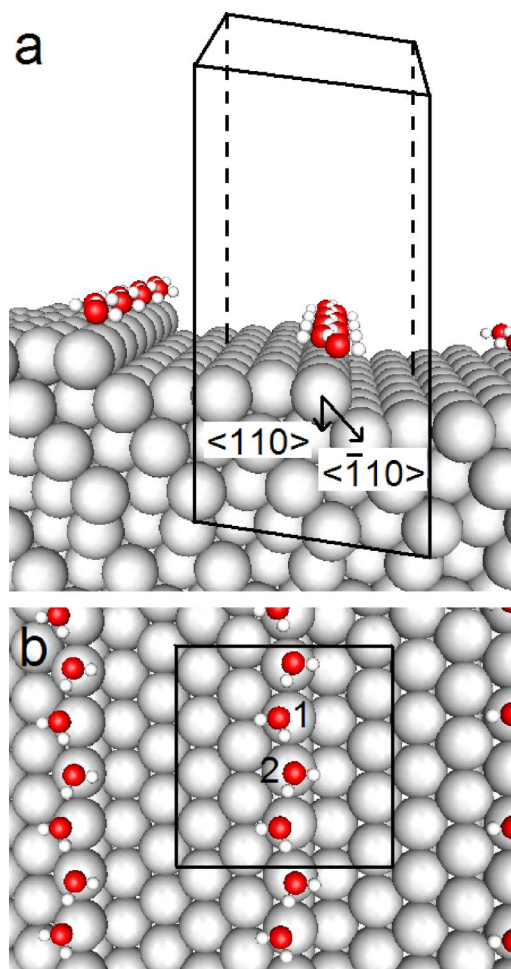
FIG. 4. The 1D water chains at a $\langle 110 \rangle / \{100\}$ step on the Pt surface, as shown by the side view (a) and the top view (b). The unit cell contains 15 layers of Pt atoms in a (322) surface.

and H-out configurations are also obtained. The last row is for the isolated monomer and the zigzag chain adsorbed on the terrace.

The isolated monomers at the two configurations bind strongly to the Pt step, with adsorption energies E_a =449 meV for H-in, and 426 meV for H-out. Among the three chains studied, only the zigzag chain is found to be stable with a binding energy of 480 meV per molecule. The H-in and H-out chains, whose adsorption energies are 431 and 385 meV, respectively, are unstable, when comparing to the corresponding monomers. The H-bond energy of the zig-

TABLE V. The water monomer and 1D chains adsorbed at the $\langle 110 \rangle / \{100\}$ step on the Pt(111) surface, modeled by an unit cell in the (322) surface.

	Monomer		1D chain	
	d_{OPt} (Å)	E_a (meV)	d_{OPt} (Å)	E_a (meV)
H-in	2.22	449	2.42	431
H-out	2.25	426	2.48	385
Mixed			2.45	480
On terrace	2.43	291	2.62, 2.72	246
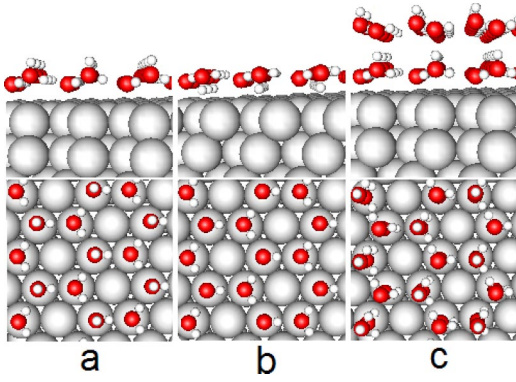
FIG. 5. (a) The H-up, (b) H-down bilayers, and (c) the double bilayers in the $\sqrt{3} \times \sqrt{3} R 30°$ symmetry on Pt(111). Both the side and top views are shown.

FIG. 6. (a) The $\sqrt{39} \times \sqrt{39} R 16.1°$ (RT39, H-down) bilayer and its atomic density profiles along the z axis for (b) O and (c) H atoms. (d) The $\sqrt{37} \times \sqrt{37} R 25.3°$ (RT37, H-down) bilayer and its density profiles for (e) O and (f) H atoms. Solid and dashed circles indicate the H_3O and OH sites, respectively. For comparison, the density profiles for the $\sqrt{3} \times \sqrt{3} R 30°$ (RT3) bilayer (H-down) are also shown by the gray lines.

zag chain can be deduced as 85 meV. This chain is stable because it favors intermolecular H bonding and the dipole-dipole interactions.[17] In addition, water monomers at the step are much more stable than those on the Pt(111) terrace (E_a = 291 meV). The zigzag chain at the step is about ~230 meV more stable than the same chain on the terrace. Such comparison suggests that water-Pt interaction is generally stronger at the steps. It explains why the water chains were only observed at the steps in experiments. The open electronic structure of the steps is responsible for the stronger interaction with water for both chains and monomers. This conclusion is in agreement with experimental observations.

4. 2D overlayers on Pt(111): the RT3, RT37, and RT39 phases

Water forms bilayers and multilayers at higher coverages. On Pt(111), different overlayers have been observed. One of the well-known forms is the $\sqrt{3} \times \sqrt{3} R 30°$ (RT3) bilayer, in which water molecules form a puckered hexagonal network, as Doering and Madey proposed.[5] However, this RT3 phase was only observed in finite domains by LEED experiment at 85 K.[32] In addition, two complex phases, $\sqrt{39} \times \sqrt{39} R 16.1°$ (RT39) and $\sqrt{37} \times \sqrt{37} R 25.3°$ (RT37) bilayers, were also observed at temperatures above 135 K.[13,9] The RT39 structure was found to transform into RT3 at ca. five bilayers.[9] Controversy still exists in the literature regarding the bilayer structure of water on Pt(111).

Figure 5 shows the structure of the RT3 bilayer in a $\sqrt{3} \times \sqrt{3} R 30°$ surface unit cell with two water molecules in each cell. The H_2O molecule in the lower plane binds directly to the surface, while the upper one forms H bonds to the molecules in the lower plane and molecules in neighboring unit cells. Three of the four H atoms form hydrogen bonds, while the fourth is either free [H-up case, panel (a)] or binds to the surface [H-down case, panel (b)]. The vertical distances between the two oxygens are 0.63 Å and 0.35 Å for the H-up and H-down bilayer, respectively (see Table VIII). Both structures are contracted compared to the bulk ice Ih with z_{OO}=0.97 Å. The adsorption energies are 522 and 534 meV, for H-up and H-down cases, respectively. The potential barrier for H-up flipping to H-down bilayer is 76 meV, as

calculated by the nudged elastic band method. This barrier is further discussed in Sec. IV C. Both structures can be candidates for bilayer on the Pt(111) surface. In comparison, the adsorption energy for the half-dissociated bilayer, the same structure suggested for Ru(0001),[10] is 291 meV, and is much smaller than those of the molecular bilayers shown in Fig. 5. Therefore, dissociation is not favored on Pt surface in RT3. Such a molecular bilayer was suggested earlier by ultraviolet photoemission spectroscopy,[37,38] the low-energy electron-diffraction measurement,[3,32] and recently by x-ray absorption spectroscopy.[15]

The $\sqrt{39} \times \sqrt{39} R 16.1°$ (RT39) and $\sqrt{37} \times \sqrt{37} R 25.3°$ (RT37) (Refs. 13 and 9) phases are also investigated. Their gross structures look very similar to that of the RT3 bilayer, i.e., puckered hexagonal networks (Fig. 6). However, the RT39 bilayer shows a quite disordered atomic distributions due to compression (by 3.3%) in the 2D unit cell. The height-dependent density profile along the surface normal (z direction) for O and H atoms are shown in the right panels of Fig. 6. Compared to the RT3 phase, in which the two O atoms are located at two positions, the density distributions of the RT39 show broadened peaks with some atoms located far away from the surface. These broadened peaks are signatures of disorder. Among the 32 water molecules in the unit cell, the lowest O atom is only 2.10 Å from the surface, while the highest H_2O is 4.4 Å above the surface, giving a rough bilayer with vertical thickness of 2.3 Å. Such a disordered bilayer is in sharp contrast to the picture of a flat bilayer proposed recently,[15] which claimed that the vertical thickness between the upper and lower O atoms is as small as 0.25 Å. The 2D lattice of the RT37 bilayer is expanded slightly by 4.4%, compared to the bulk ice Ih, as in the RT3 (7.2%) phase. It is also disordered, but not as
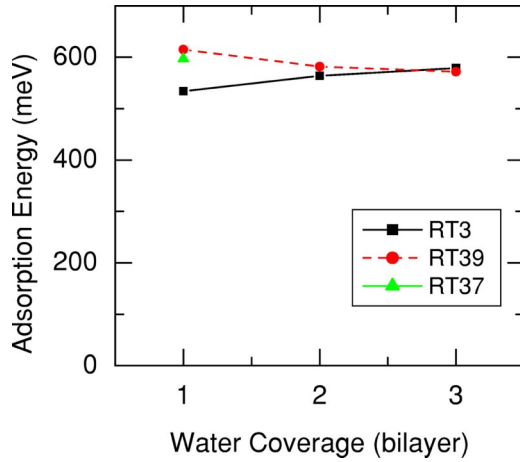
FIG. 7. The adsorption energy of various overlayer phases on Pt(111) at coverages from 1 to 3 bilayers. The square, circle, and triangle represent the $\sqrt{3} \times \sqrt{3} R 30°$ (RT3), the $\sqrt{39} \times \sqrt{39} R 16.1°$ (RT39), and the $\sqrt{37} \times \sqrt{37} R 25.3°$ (RT37) structures, respectively.

much as the RT39 (Fig. 6). The maximum O-Pt distance in the RT37 is 3.58 Å, similar to that in the RT3 bilayers, 3.37 Å (H-up) and 3.14 Å (H-down). One key feature of the RT39 structure is the existence of a few H_3O^+ like (i.e., dissociated) molecules, which will be discussed further in Sec. IV D.

To see the coverage dependence of the structure and energetics in the overlayers, water in the RT3 phase has been studied from two bilayers, Fig. 5(c), to six bilayers. The O-O distance between two adjacent bilayers is 2.75–2.83 Å. The water-metal bond for the bottom molecule decreases gradually. The adsorption height of the bottom water equals 2.69, 2.63, 2.56, 2.49, 2.52, and 2.47 Å, respectively, when the coverage goes from one to six bilayers. In contrast, the height of the upper water in the first bilayer remains almost constant, 3.25±0.02 Å. This indicates that in bilayer and multilayers, only molecules in the bottom have a direct interaction with the metal surface (see Fig. 5), while the upper molecule is almost unaffected, suggesting that the water-surface interaction on Pt(111) is rather localized.

Figure 7 compares the adsorption energy of the RT3 and RT39 phases for up to three bilayers. It shows that the adsorption energy of the RT39 phase, 615 meV, is slightly more favorable (by 80 meV) compared to the RT3 phase, 534 meV, at one bilayer coverage. The adsorption energy for the RT37 phase, 597 meV, lies in between. As the coverage increases, the RT3 phase becomes more favorable compared to other two phases, as found in recent experiment. The RT39 phase was found to transform into RT3 after a structural reorientation[9] at about five bilayers, as estimated from the same experiment.

Information concerning the detailed structures and bonding information for all the calculated overlayers on Pt(111) are summarized in Table VI.

B. Water on different metal surfaces

Here below, we extend our study to other metal surfaces such as Au, Pd, Rh, and Ru, which have been under experi-

TABLE VI. The structures and energetics for water clusters and thin films on the Pt(111) surface. The unit cell, the number of molecules n, the number of H_2O-metal bonds $N_{H_2O\text{-}M}$, and the number of H bonds N_{HB} in the unit cell are shown together with the adsorption energies E_a, and the H-bond energies E_{HB} (in meV). The two energies for the bilayer correspond to the H-up/H-down cases.

Ads. species	Unit cell	n	E_a	$N_{H_2O\text{-}M}$	N_{HB}	E_{HB}
Monomer	3×3	1	304	1	0	
Dimer	3×3	2	433	2	1	258
Trimer	3×3	3	359	3	3	55
Hexamer	$2\sqrt{3} \times 2\sqrt{3}$	6	520	3	6	368
Bilayer	$\sqrt{3} \times \sqrt{3}$	2	505/527	1	3	235
Two bilayers	$\sqrt{3} \times \sqrt{3}$	4	564	1	7	312
Three bilayers	$\sqrt{3} \times \sqrt{3}$	6	579	1	11	303
Four bilayers	$\sqrt{3} \times \sqrt{3}$	8	588	1	15	307
Five bilayers	$\sqrt{3} \times \sqrt{3}$	10	593	1	19	307
Six bilayers	$\sqrt{3} \times \sqrt{3}$	12	601	1	23	320
Bilayer	$\sqrt{37} \times \sqrt{37}$	26	597	13	39	297
Bilayer	$\sqrt{39} \times \sqrt{39}$	32	615	16	48	309
Two bilayers	$\sqrt{39} \times \sqrt{39}$	64	582	16	112	275
Three bilayers	$\sqrt{39} \times \sqrt{39}$	96	572	16	176	276

mental investigation. The closely packed surfaces, i.e., the (111) for the fcc and (0001) for the hcp metals, were chosen for comparison. These surfaces differ from Pt(111) in two aspects: (i) the variation of the surface lattice constant, which matches differently with the H-bonded water networks; and (ii) the change in the chemical reactivity associated with the variation of the d-band occupancy. Our basic concern is whether and how these two factors, geometry and chemical reactivity, affect the water structures and properties at surfaces. What are the general trends of water-surface interactions. To this end, we consider only two prototype structures, the monomers and bilayers. The former is ideal for the calibration of the metal-surface coupling, while the bilayer enables us to examine both the water-surface and the interwater interactions.

1. Water monomers on Ru, Rh, Pd, Pt, and Au

The structure of the water monomer on these surfaces has been investigated in detail in a recent study.[31] The structure of water monomer on Pt(111) seems to be general to all these surfaces.[31] Results for monomer on these surfaces from our calculation are given in Table VII. Top site adsorption is most stable on all these surfaces, with $\theta = 6°$–$24°$. An increased OH bond and a more open HOH angle are generally found. This indicates electron transfer from the O to the surface, as we found on the Pt(111) surface.

Regarding the differences and details, the interaction of water with Ru and Rh is found to be much stronger than the Pt and Pd, while it is much weaker on the Au surface. The adsorption energetics suggests a bonding order as Ru>Rh >Pd>Pt>Au, This is further supported by the trend in the d_{OM} and the bonding angles, θ and $\angle$HOH. This bonding order reflects the chemical reactivity of these surfaces, as

TABLE VII. Geometries and energetics of a water monomer on the Ru(0001), Rh(111), Pd(111), Pt(111), and Au(111) surfaces. Energies, distances, and angles are in units of meV, Å, and deg, respectively.

Substrate	Layer	Top		Bridge		Hollow		d_{OH}	$\angle HOH$	θ
		d_{OM}	E_a	d_{OM}	E_a	d_{OM}	E_a			
Ru(0001)	5	2.28	409	2.55	92	2.56	67	0.981	105.66	16
Rh(111)	4	2.32	408	2.57	126	2.70	121	0.978	105.95	24
Pd(111)	4	2.42	304	2.74	146	2.77	130	0.977	105.63	20
Pt(111)	4	2.43	291	3.11	123	3.12	121	0.978	105.36	13
Au(111)	7	2.67	105	2.80	32	2.80	25	0.977	105.04	6

indicated by the periodic table. Our results are largely consistent with those by Michaelides and co-workers,[31] although some details differ. For example, the monomer adsorption energy was ordered as Rh>Ru>Pt>Pd>Au in their results. However, the energy difference between Ru and Rh and the difference between Pt and Pd, are very small. In fact they are within the accuracy of the calculations.

2. Water bilayers on different surfaces

To examine the H bonding on different surfaces, water in the $\sqrt{3} \times \sqrt{3} R30°$ bilayer has been calculated on different surfaces. Structure parameters and adsorption energies are summarized in Table VIII. The puckered hexagonal network on these surfaces is very similar to the RT3 bilayer on Pt(111). The adsorption height of the bottom water z_{OM1} increases gradually in the order of Ru>Rh>Pd>Pt>Au, as in the periodic table, while the height of the upper water z_{OM2} keeps almost constant, namely, 3.40 Å for H-up and 3.20 Å for the H-down bilayer. The vertical O-O distance z_{OO} decreases therefore along this order. These results are more clearly shown in Fig. 8 for the H-up bilayer. The results for the H-down bilayer look very similar and are not shown

here. The universal structure of the upper water layer indicates that the water-surface interaction is localized dominantly in the bottom layer, while the molecules in the upper layer are almost unaffected.

The bonding order shown above correlates directly with the d-band filling of these surfaces, which increases accordingly along the periodic table. The d-band occupation is well known to affect atomic adsorption for the H and O atoms, and the general activity of the metal surfaces. From Fig. 8, we can also conclude that the d-band occupancy has a direct effect on the water-surface bonding properties. We believe that the effect of the 2D lattice constant, which also increases from Ru (2.72 Å) to Au (2.95 Å), has a smaller and indirect effect on the interaction with water.

In addition to the RT3 bilayer, half-dissociated bilayer proposed by Feibelman has also been calculated on these surfaces. The two O-M bond lengths are 2.10 and 2.20 Å (except for Au), and are much shorter than those in the molecular bilayer. It is a very flat overlayer ($z_{OO} \sim 0.05$ Å). However this structure is only energetically favorable on Ru(0001). On Au(111), it is completely repulsive.

TABLE VIII. The geometries and energetics for the H-up, the H-down, and the half-dissociated water bilayers adsorbed on different metal surfaces. Here z_{OO}, z_{OM1}, and z_{OM2} are the vertical distances between the top and bottom O atoms, the bottom O and the underlying metal atom, and the top O and the metal atom, respectively.

Surface	Bilayer	z_{OO} (Å)	z_{OM1} (Å)	z_{OM2} (Å)	E_a (meV/molecule)
Ru(0001)	H-up	0.86	2.46	3.42	531
	H-down	0.42	2.69	3.22	533
	Half-disso.	0.05	2.09	2.16	766
Rh(111)	H-up	0.79	2.50	3.40	562
	H-down	0.42	2.52	3.12	544
	Half-disso.	0.04	2.09	2.16	468
Pd(111)	H-up	0.60	2.78	3.45	530
	H-down	0.36	2.66	3.18	546
	Half-disso.	0.07	2.09	2.20	89
Pt(111)	H-up	0.63	2.70	3.37	522
	H-down	0.35	2.68	3.14	534
	Half-disso.	0.06	2.12	2.23	291
Au(111)	H-up	0.46	2.90	3.38	437
	H-down	0.29	2.85	3.25	454
	Half-disso.	0.14	2.20	2.43	-472
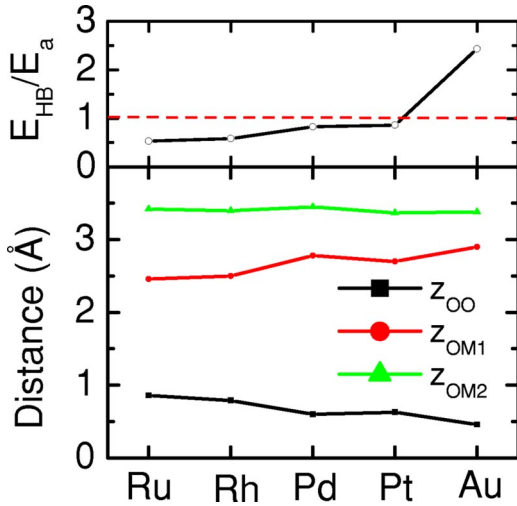
FIG. 8. The structure parameters (z_{OO}, z_{OM1}, z_{OM2}) and the wettability, defined as $w = E_{HB}/E_a$, for an H-up bilayer on the Ru(0001), Rh(111), Pd(111), Pt(111), and Au(111) surfaces. The case for the H-down bilayer is very similar.

Recent experiments seem to favor the H-down bilayer on Pt(111) (Ref. 15) and Ru(0001).[18] These experiments are consistent with our calculations, although the H-down bilayer is only a few tens of meV favorable on Pt. Interestingly, our calculation suggests that the H-up bilayer is more favorable than the H-down bilayer on Rh(111), although no direct comparison with experiment has yet been possible.

3. The wetting order of the metal surfaces

With the results of the adsorbed monomers and bilayers available, we now concentrate on a specific issue of water-surface interaction at surfaces, namely, the wettability of a surface. This question is general and important to both the fundamental understanding of the water-solid interactions and to technological applications such as biosensor and waterproof materials. Experimentally, the wettability of a surface has been characterized macroscopically by the contact angle at the interfaces. In a recent study,[19] we have proposed a molecular picture of wettability, which is simply defined as the ratio between the H-bond energy of the adsorbed water structures and the monomer adsorption energy. Such a characterization has been justified on three surfaces: Pt, Au, and graphite.[19]

The upper panel of Fig. 8 shows the so-defined wettability, $w = E_{HB}/E_a$, of these surfaces with the H-bond energies deduced from the bilayer. More explicitly, we used

$$E_{HB} = (E_a[\text{bilayer}] \times 2 - E_a[\text{monomer}])/3, \qquad (2)$$

which characterizes the mean H-bond energy in the bilayer. The smaller the w is, the stronger is the wettability of the surface. The upper panel of Fig. 8 shows an order of w as $w_{Ru} \lesssim w_{Rh} < w_{Pd} \lesssim w_{Pt} < w_{Au}$, giving a wetting order of Ru $>$ Rh $>$ Pd $>$ Pt $>$ Au. The $w = 1$ line has been suggested as the approximate border dividing the hydrophilic ($w \lesssim 1$) and hydrophobic ($w \gg 1$) surfaces. According to this, Ru, Rh, Pd, and Pt lie in the hydrophilic region. On the contrary, Au is in the hydrophobic region. This division is consistent with the experimental understanding.[39,40] The wetting order results essentially from the variation of the water-metal interaction on these surfaces, because the H-bond energy does not change appreciably on different surfaces. The trend shown in Fig. 8 also implies a general relationship between the hydrophilicity-hydrophobicity and the monomer adsorption energy. Such a relationship was independently found in a recent model study,[41] where a linear correlation between the contact angle and the monomer binding energy was established from the Monte Carlo simulations. It justifies our model of wettability, based on the parameters of molecule-surface interactions.

C. Vibrational spectra

To provide a database for vibrational recognition of water structures at the surfaces, we have carried out MD simulations to extract the vibrational spectra for the adsorbed structures. Vibrational spectra has been quite useful for the identification of surface and interface structures, because they are measurable by experiments.

For comparison with experiments, we have calculated the spectra for water monomers, dimers, and bilayers on Pt(111); bilayers on Pd(111), Rh(111), and Au(111); and H-up, H-down, and half-dissociated bilayers on Ru(0001). The eigenfrequencies for the adsorbed structures are listed in Table IX. These spectra are generally characterized by three regions: (A) the low-energy modes below 120 meV, which correspond to the translational and librational motions; (B) The HOH bending modes at ~ 200 meV; and (C) the OH stretch modes between 300 and 470 meV. On Pt(111) surface, an excellent agreement was found between the calculated spectra and the EELS and HAS data for the RT3 bilayer.[14] On Ru(0001), the vibrational spectra seems to match better with that of the H-up bilayer, an issue discussed by a recent experiment.[18]

The vibrational spectra also enable us to estimate the effect of zero point energy on the adsorption energetics. For instance, the zero-point energy ($E_{zp} = \Sigma_i \hbar w_i/2$) is ~ 90 meV per molecule for the first bilayer on Pt(111). It stabilizes the bilayer by 30 meV compared to ice Ih, whose E_{zp} is 120 meV. Such estimation can be applied to other cases, as soon as the zero-point energy is of concern.

IV. DISCUSSION ON A FEW TOPICS

With the results presented in the preceding section, we now turn to discuss a few specific topics, which are central to the water-metal interactions and the interface properties. We bring up this discussion because the understanding on these issues are so far not yet conclusive. Although the discussions here are made on specific structures and systems, we try to point out their possible implications on other systems and processes.

A. The nature of the water-surface bond

First of all, we discuss the nature of the water-surface bond. This issue is relevant and important because there are general concerns about the character of the water-surface bond, due to the dipole moment of water molecules.

TABLE IX. The calculated and experimental vibrational energies for the water bilayers on the Pt(111), Pd(111), Rh(111), Au(111), and Ru(0001) surfaces (in meV). See Refs. 12,14,32 for the assignment of these modes.

Substrate		Translations and librations						δ_{HOH}	$\nu_{O\text{-}HB}$	$\nu_{O\text{-}H}$
Ru(0001)	H-up	34	40	50	67	87	119	200	378, 424	462
	H-down	20	48	61	73	89	111, 129	196	347, 440	440
	Half-disso.	20	32	53	77		117, 129	186, 196	300–380, 428	
	Expt.[a]		48		68	87	114	189	364, 422, 442	457
	Expt.[b]								384, 427	457
Rh(111)	H-up	18	44		61	89	111, 129	198	349, 422	466
	H-down	20	44		75	89	133	200	347, 420	440
Pd(111)	H-up	14	40	53	67	89	109, 117	198	374, 424	466
	H-down	20	42	57	71	89	111, 123	202	380, 426	444
Pt(111)	monomer	16		40	61	89	113, 121	190		440
	dimer	20	32	44	65	85	105, 133	198	347	432, 452
	H-up	18	32	53	69	87	107, 119	198	388, 432	467
	H-down	16	34	57	69	91	111, 119	196, 202	384, 424	438
	Expt.[c]	16.5	33	54	65	84	115, 129	201	424	455
Au(111)	H-up	17	36				108	201	400, 444	466
	H-down	18	36		77		105	202	402, 436	468
	Expt.[d]		31				104	205	409	(452)[e]

[a]Ref. 42.

[b]Multiple by an isotope factor 1.35 from D_2O/Ru(0001) (Ref. 18).

[c]Ref. 32 and 43.

[d]Ref. 12.

[e]Taken from water/Ag(111) (Ref. 44).

The dipole-dipole interaction of van der Waals (vdW) type has been believed to play a role in the water-surface interactions. Indeed, vdW has been found to be crucial for the weakly interacting surfaces, such as water on graphite.[45]
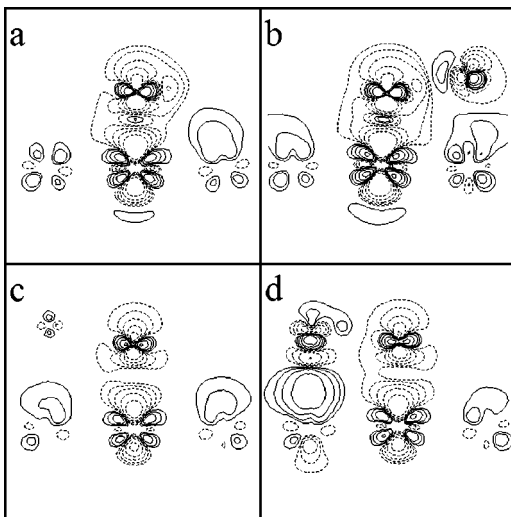
FIG. 9. Isodensity contours of the difference electron density for (a) the water monomer, (b) the dimer, (c) the H-up bilayer, and (d) the H-down bilayer on Pt(111). The difference density is defined as $\Delta\rho = \rho[(H_2O)_n /Pt] - \rho[(H_2O)_n] - \rho[Pt]$. Here n is the number of H_2O molecules in the unit cell. The contours have densities $\Delta\rho = \pm 0.005 \times 2^k e/$ Å^3, for $k = 0, 1, 2, 3, 4$. Solid and dashed lines correspond to $\triangle\rho > 0$ and $\triangle\rho < 0$, respectively.

To see the nature of the water-surface bond, Fig. 9 shows the difference electron density for a water monomer, a dimer, the H-up and H-down bilayers on the Pt(111) upon adsorption. The horizontal axis is in the [110] direction, and also goes approximately along one of the OH bonds, while the vertical axis is normal to the surface. The induced densities in Fig. 9 exhibit a d_{xz} and d_{z^2} character for all the calculated structures on the Pt(111). It indicates that the d bands, especially the surface states of d_{xz} and d_{z^2} characters, of Pt(111), are generally involved in the water-Pt interactions, which leads to ~ 0.02 electron transfer from O to Pt. The H-O-H binding is weakened, as observed by the OH elongation and HOH widening, due to the reduced bonding electrons in water. This picture is consistent with earlier studies[46,47] of water on other surfaces, where the lone pair–d band coupling was found to be crucial for the molecule-surface interaction.

Figure 9 also shows that the water-surface bonding is rather localized in the bottom layer, as shown clearly in Figs. 9(c) and 9(d). The upper molecule of the RT3 bilayer shows very little coupling to the surface. This led us to the conclusion that *the water at surfaces forms chemical bond with metal electrons, especially with those of the surface states. This water-surface bond is rather localized at the interfaces, and mostly in the bottom layer of molecules.* Similar conclusion has recently been drawn by Michaelides and co-workers.[47]

The chemical bonding between water and the surfaces often induces electron transfer. Figure 10 shows the work
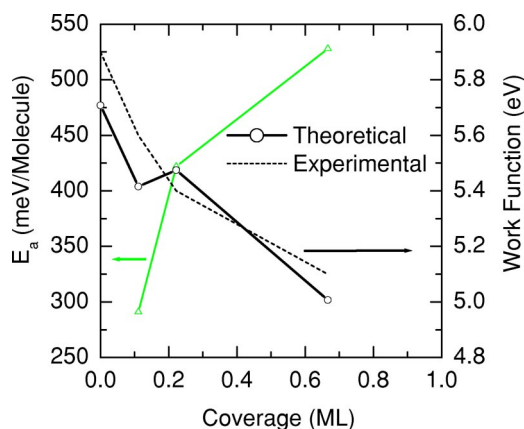
FIG. 10. The work function change for water/Pt(111) upon adsorption.

FIG. 11. The minimum energy pathway (MEP) and the transition state between the H-up and H-down bilayers on Pt(111).

function change of the Pt(111) surface adsorbed with H_2O monomers, dimers, and bilayers (averaged over the H-up and H-down cases). The size of the unit cells used in the calculations provides an approximate calibration of adsorbate coverages, which are 1/9, 1/3, and 2/3 monolayers (ML), respectively. The mean adsorption energy is also plotted for comparison. Water adsorption results in a reduction of the work function from 5.8 eV to 5.0 eV. In experiments, a monotonic decrease of work function was measured for up to the formation of a bilayer,[48] with 0.7–0.8 eV decrease at one bilayer. This reduction of the work function is a clear indication of the electron transfer from water to the surface, a picture consistent with the induced electron densities shown in Fig. 9.

B. The enhancement of hydrogen bonding at surfaces

As a related issue, the interwater interaction, namely, the H bonding in the interface structures is another issue of general interest. In principle, H bonding at surfaces is strongly entangled with the water-surface interactions, especially in small nanostructures and clusters, where a clear separation of the two interactions is difficult. However, a qualitative picture of the H bonding at surfaces is still important and relevant for a number of issues related to interface water.

Water adsorption strengthens the H bonding. This can be seen from the adsorbed dimer, the simplest H-bonded system at surfaces. From Table IV, the H-bond energy in the adsorbed dimer on Pt can be estimated, by subtracting one or two monomer adsorption energy, to be between 258 ($433 \times 2 - 304 \times 2$) and 562 ($433 \times 2 - 304 \times 1$) meV, which is larger than the bond strength of the free dimer, 250 meV. This enhancement is unusual because it does not agree with the Pauling's principle for chemical bonding, according to which the H bond of water molecules should be weakened when more bonds, here the water-surface bonds, form. Enhancement of H bonding can generally be seen in other structures, as shown by the last column of Table VI, except for the adsorbed trimers. In the latter case, the seemingly weakened H-bonding is an artifact of our bond counting. We counted three water-Pt bonds plus three H bonds in the tri-

mers, where in reality the H bonds and water-surface bonds are closely entangled.
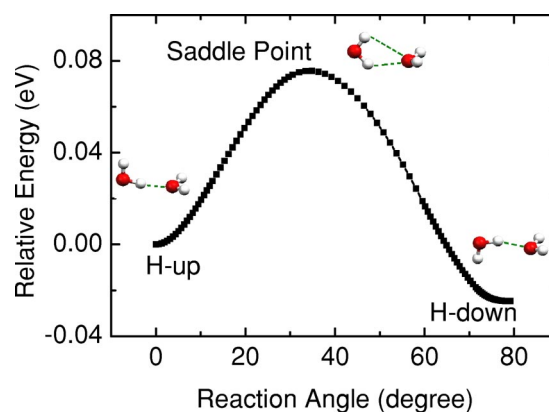
The enhancement of H bonding by the metal substrates can be directly seen by the valence charge redistribution, as shown for water/Pt(111) in early publication.[14] This H-bond enhancement has generally been observed on other substrates including Pd, Rh, Ru, and Au. It is worth mentioning that H-bonding enhancement was also found in water clusters and bulk water.[49]

C. The H-up and H-down conversion in the RT3 bilayer

The two bilayers in the RT3 phase on Pt, the H-up and H-down cases, are nearly degenerate in adsorption energies, 522 and 534 meV, respectively (see Table VII). The 2D structures of both bilayers have nearly the same oxygen arrangement. They are therefore indistinguishable, as soon as the measurements are not sensitive to the positions of the H atoms, which is true for most experiments. It is therefore intriguing to ask what is the barrier between the two states. Are the two states distinguishable or are they in fact the same state? The answer to this question depends critically on the energy barrier between the two states and the nature of the H-atom motion around the barrier. A full account of this issue requires a quantum-mechanical treatment of the H atoms along the minimum energy path (MEP). Here, our discussion relies fully on the classical treatment of the H atoms and the DFT calculations of the electrons.

The calculated MEP and the schematic transition state (saddle point) are shown in Fig. 11. The MEP involves mainly the rotation of the upper H_2O molecule in the HOH plane. The potential barrier for H-up flipping to H-down bilayer is found to be 76 meV at the reaction angle $\simeq 33°$, corresponding to OH angle relative to the surface normal. This barrier is substantially lower than the corresponding barrier, 300 meV, on Ru(0001).[47] But it agrees well with the barrier for similar conformational change in a free dimer, 78 meV (Ref. 50) (the energy difference between structures 1 and 9 in Fig. 2 there). In this sense, the presence of the Pt(111) surface has little influence on this barrier. This is consistent with the fact that the barrier is located well above the bottom water plane, where the interaction with the surface is predominant. It would be interesting to find out how this barrier changes in a quantum-mechanical treatment of the H atoms.[51]

D. Partial dissociation of water bilayers

A recent experiment[18] questioned the existence of a half-dissociated water adlayer on Ru(0001), proposed by Feibelman. It is therefore interesting to look at the kinetic constraints for the dissociation and other competing processes such as molecular desorption. The barrier for dissociation from the H-down bilayer to the half-dissociated structure is 0.62 eV, as found in another calculation.[31] However the adsorption energy of the RT3 bilayer is 0.53 eV according to our calculation, which implies that water in the bilayer is easier to desorb than to dissociate. The higher barrier for dissociation may thus completely prohibit the existence of any dissociated water on Ru, as found in experiments at $\sim$ 140 K.

Partial dissociation of H_2O molecules have also been found in the RT39 phase,[16] forming H_3O^+ and OH^- like groups on Pt(111), although the fraction of dissociated molecules is very small. From our calculation, we found three dissociated molecules out of 32 (9%) in the first RT39 bilayer, with all H_3O^+ lying in the upper layer and the OH^- lying in the bottom layer. When the water film grows thicker, less dissociation is found: only 2 out of 64 (3%) molecules in two bilayers and 1 out of 96 (1%) in three bilayers. Contrary to the RT39 phase, no dissociation is found in the RT3 and RT37 bilayers.

The partial dissociation of the RT39 bilayer on Pt(111) results from both lateral compression of the water film and its interaction with the substrate. This is evidenced by the fact that if we remove the Pt substrate, one and only one H_2O dissociates, compared to three in the first bilayer on Pt. Further evidence for surface induced dissociation comes from the fact that only the bottom H_2O molecules donate protons, indicating the influence of the substrate. In contrast, none of the upper H_2O (H-down) molecules is found to donate a proton to other H_2O. Therefore all the H_3O^+s lie in the upper layer of the first bilayer while the OH^-s bind to the Pt surface with a Pt-O bond length of 2.1 Å. Lateral compression also contributes to partial dissociation, because one water molecule is dissociated in the RT39 even in the absence of the surface, and because the RT37 or RT3 phases do not exhibit any dissociation. Compression induced dissociation is a well-known phenomenon in bulk water[52] and thin films.[53] The effect of compression in the RT39 bilayer provides a surface example of this general phenomenon in a two-dimensional system.

V. SUMMARY AND CONCLUSIONS

The adsorption of water on metal surfaces has been investigated by *ab initio* DFT calculations. From these studies, the following conclusions can be drawn.

(i) The interaction between water and metal surfaces is dominated by a chemical bonding formed between the lone pair of water molecules and the surface electronic states. As a result, the water-surface bond is rather localized, mostly in the contacting regions and bottom layers like, for example, the donor of the dimer, and the bottom molecule in the bilayer. Long-range polarization does exist, however, its effect is relatively smaller.

(ii) An enhancement of the interwater H bonding has been generally observed in both nanometer clusters and overlayers. This enhancement is especially obvious in small clusters such as the dimer and in the first bilayers. We would like to point out that such an enhancement is not consistent with Pauling's principle for chemical bonds, but seems to be a unique feature of the H-bonded water molecules.

(iii) The structure of water in the adsorbed states remain largely the same as the gas-phase or bulk ice counterparts. Although water molecules do adjust their bonding features, like the bond lengths and angles, upon adsorption. On the surfaces with strong water-metal coupling, like Ru, Rh, such adjustment is more significant. It is minor on the weakly interacting systems such as Au. In the latter case, water structures remain largely rigid. This reflects the competition between the two fundamental interactions in the adsorbed water molecules. In this sense, water could also be hard.

(iv) The wetting order of the studied surfaces is found as Ru>Rh>Pd>Pt>Au, the same order as the *d*-band occupancy of the metals. This ordering results from the chemical reactivity of the substrates, and is a direct indication of the localized electronic coupling between water and the substrates.

(v) Vibrational spectra of various water structures are obtained and are generally consistent with the structures and interactions present upon adsorption. These vibrational spectra, in particular the OH stretch modes, provide a useful database for vibrational recognition of interface structures by experiments.

The results presented in this paper, based on the DFT calculations, gained much insight into the fundamental water-metal interactions at the atomic to electronic scales. Detailed characterization of the prototype water structures on several metal surfaces has been documented and a comprehensive understanding of the water-metal interactions has emerged. We believe that such an understanding is generalizable to other surfaces. Nevertheless, one should be aware of the fact that some important aspects of water-surface interactions have not been tackled and are beyond the theoretical approach we adopted here. These include, for example, the quantum-mechanical character of H-atom motion in water; the kinetic and thermodynamical effects such as entropy, temperature, and pressure; and the possible dispersive forces such as the van der Waals interactions. These issues deserve our attention in future studies.

[1] P.A. Thiel and T.E. Madey, Surf. Sci. Rep. **7**, 211 (1987).

[2] M.A. Henderson, Surf. Sci. Rep. **46**, 1 (2002).

[3] M. Morgenstern, T. Michely, and G. Comsa, Phys. Rev. Lett. **77**, 703 (1996); M. Morgenstern *et al.*, Z. Phys. Chem. (Munich) **198**, 43 (1997).

[4] L.E. Firment and G.A. Somorjai, J. Chem. Phys. **63**, 1037 (1975); Surf. Sci. **84**, 275 (1979).

[5] D.L. Doering and T.E. Madey, Surf. Sci. **123**, 305 (1982).

[6] K. Morgenstern and J. Nieminen, Phys. Rev. Lett. **88**, 066102 (2002).

[7] K. Morgenstern and K-H. Rieder, J. Chem. Phys. **116**, 5746 (2002).

[8] T. Mitsui, M.K. Rose, E. Fomin, D.F. Ogletree, and M. Salmeron, Science **297**, 1850 (2002).

[9] S. Haq, J. Harnett, and A. Hodgson, Surf. Sci. **505**, 171 (2002).

[10] P.J. Feibelman, Science **295**, 99 (2002); D. Menzel, *ibid.* **295**, 58 (2002).

[11] K.D. Gibson, M. Viste, and S.J. Sibener, J. Chem. Phys. **112**, 9582 (2000).

[12] G. Pirug and H.P. Bonzel, Surf. Sci. **405**, 87 (1998).

[13] A. Glebov, A.P. Graham, A. Menzel, and J.P. Toennies, J. Chem. Phys. **106**, 9382 (1997).

[14] S. Meng, L.F. Xu, E.G. Wang, and S.W. Gao, Phys. Rev. Lett. **89**, 176104 (2002).

[15] H. Ogasawara, B. Brena, D. Nordlund, M. Nyberg, A. Pelmenschikov, L.G.M. Pettersson, and A. Nilsson, Phys. Rev. Lett. **89**, 276102 (2003).

[16] P.J. Feibelman, Phys. Rev. Lett. **91**, 059601 (2003).

[17] D.J. Mann and M.D. Halls, Phys. Rev. Lett. **90**, 195503 (2003).

[18] D.N. Denzler, Ch. Hess, R. Dudek, S. Wagner, Ch. Frischkorn, M. Wolf, and G. Ertl, Chem. Phys. Lett. **376**, 618 (2003).

[19] S. Meng, E.G. Wang, and S.W. Gao, J. Chem. Phys. **119**, 7617 (2003).

[20] G. Kresse and J. Hafner, Phys. Rev. B **47**, 558 (1993); **49**, 14251 (1994); J. Phys.: Condens. Matter **6**, 8245 (1994); G. Kresse and J. Furthmüller, Comput. Mater. Sci. **6**, 15 (1996); Phys. Rev. B **54**, 11169 (1996).

[21] H.J. Monkhorst and J.D. Pack, Phys. Rev. B **13**, 5188 (1976).

[22] M. Methfessel and A.T. Paxton, Phys. Rev. B **40**, 3616 (1989).

[23] H. Jonsson, G. Mills, and K.W. Jacobsen, in *Classical and Quantum Dynamics in Condensed Phase Simulations*, edited by B.J. Berne, G. Ciccotti, and D. F. Coker (World Scientific, Singapore, 1998).

[24] D. Vanderbilt, Phys. Rev. B **41**, 7892 (1990).

[25] J.P. Perdew, J.A. Chevary, S.H. Vosko, K.A. Jackson, M.R. Pederson, D.J. Singh, and C. Fiolhais, Phys. Rev. B **46**, 6671 (1992).

[26] L. Giordano, J. Goniakowski, and J. Suzanne, Phys. Rev. Lett. **81**, 1271 (1998).

[27] S. Tsuzuki and H.P. Lüthi, J. Chem. Phys. **114**, 3949 (2001).

[28] F. Sim, A. St-Amant, I. Papai, and D.R. Salahub, J. Am. Chem. Soc. **114**, 4391 (1992).

[29] R.N. Barnett and U. Landman, Phys. Rev. B **48**, 2081 (1993).

[30] S. Izvekov and G.A. Voth, J. Chem. Phys. **115**, 7196 (2001).

[31] A. Michaelides, V.A. Ranea, P.L. de Andres, and D.A. King, Phys. Rev. Lett. **90**, 216102 (2003).

[32] K. Jacobi, K. Bedürftig, Y. Wang, and G. Ertl, Surf. Sci. **472**, 9 (2001).

[33] M. Nakamura, Y. Shingaya, and M. Ito, Chem. Phys. Lett. **309**, 123 (1999); M. Nakamura and M. Ito, *ibid.* **325**, 293 (2000).

[34] A.L. Glebov, A.P. Graham, A. Menzel, Surf. Sci. **427**, 22 (1999).

[35] H. Ogasawara, J. Yoshinobu, and M. Kawai, J. Chem. Phys. **111**, 7003 (1999); Chem. Phys. Lett. **231**, 188 (1994).

[36] J.K. Gregory, D.C. Clary, K. Liu, M.G. Brown, and R.J. Saykally, Science **275**, 814 (1997).

[37] G.B. Fisher and J.L. Gland, Surf. Sci. **94**, 446 (1980).

[38] F.T. Wagner and T.E. Moylan, Surf. Sci. **191**, 121 (1987).

[39] R.S. Smith, C. Huang, E.K.L. Wong, and B.D. Kay, Surf. Sci. **367**, L13 (1996).

[40] P. Löfgren, P. Ahlström, D.V. Chakarov, J. Lausmaa, and B. Kasemo, Surf. Sci. **367**, L19 (1996).

[41] T. Werder, J.H. Walther, R.L. Jaffe, T. Halicioglu, and P. Koumoutsakos, J. Phys. Chem. B **107**, 1345 (2003).

[42] P.A. Thiel, R.A. DePaola, and F.M. Hoffmann, J. Chem. Phys. **80**, 5326 (1984).

[43] B.A. Sexton, Surf. Sci. **94**, 435 (1980).

[44] A.F. Carley, P.R. Davies, M.W. Roberts, and K.K. Thomas, Surf. Sci. **238**, L467 (1990).

[45] D. Feller and K.D. Jordan, J. Phys. Chem. A **104**, 9971 (2000).

[46] H.P. Bonzel, G. Pirug, and J.E. Müller, Phys. Rev. Lett. **58**, 2138 (1987).

[47] A. Michaelides, A. Alavi, and D.A. King, J. Am. Chem. Soc. **125**, 2746 (2003).

[48] I. Villegas and M.J. Weaver, J. Phys. Chem. **100**, 19 502 (1996).

[49] S.S. Xantheas, C.J. Burnham, and R.J. Harrison, J. Chem. Phys. **116**, 1493 (2002).

[50] B.J. Smith, D.J. Swanton, J.A. Pople, H.F. Schaefer III, and L. Radom, J. Chem. Phys. **92**, 1240 (1990).

[51] D. Marx, M.E. Tuckerman, J. Hutter, and M. Parrinello, Nature (London) **397**, 601 (1999).

[52] E. Schwegler, G. Galli, F. Gygi, and R.Q. Hood, Phys. Rev. Lett. **87**, 265501 (2001).

[53] S. Meng, E. G. Wang, and S. W. Gao (unpublished).